Power Converter Decentralized Specifications in Different Grid Nodes for DC Distribution Systems

Lazar Stojanović, *Student Member, IEEE*, Ružica Cvetanović, *Graduate Student Member, IEEE*, Paolo Mattavelli, *Fellow, IEEE*, and Simone Buso, *Member, IEEE*

***Abstract*—Impedance-based methods are commonly applied to analyze the small-signal stability of grids with numerous power electronics converters (PECs). Due to the complexity of the grid, decentralized impedance specifications—allowing independent requirements for each PEC—offer significant advantages from the system operator's perspective, especially when PECs originate from multiple vendors. In fact, by applying decentralized specifications to the targeted PECs, the system operator ensures small-signal stability regardless of the specific control design of the PEC. The article extends the existing impedance specifications by developing a new approach to impose decentralized specifications on individual PECs connected to different grid nodes. This is obtained using the Gershgorin theorem to derive analytical conditions each PEC must satisfy. Since these conditions can be overly conservative, a combination of selected condition violations and impedance-based passivity criteria is proposed. Finally, the proposed approach is experimentally validated on a dc distribution system consisting of three dc–dc buck converters. The results demonstrate that instability can occur when the converters do not meet the specified requirements, whereas stability is maintained when the specifications are satisfied.**

***Index Terms*—DC distribution systems, decentralized impedance specifications, Gerhgorin theorem, power converters, small-signal stability.**

I. Introduction

MANY stability problems have been observed due to the interactions of power electronic converters (PECs) and the grid [1], [2]. Therefore, analyzing and mitigating these interactions is crucial for system reliability and robustness. Although the systems involving PECs are nonlinear, a lot of destabilizing interactions can be analyzed based on the system's linearized representation around an operating point [2], [3], [4]. By relying on such a representation, this article addresses small-signal stability analysis, leaving the large-signal stability analysis outside of its scope. An effective way to study PECs' small-signal interactions is the impedance-based approach. Typically, this approach is applied at a certain interface, i.e., point-of-connection [4], [5], [6]. For this, the system under study is partitioned into two subsystems. For example, in [5], the two subsystems are the converter and the rest of the system (grid) to which it is connected. These subsystems are then represented by their small-signal Norton/Thevenin equivalents. Finally, the stability is assessed by applying the (generalized) Nyquist criterion to the minor loop gain, which is the product/ratio of the subsystems' impedances/admittances, jointly referred to as immittances.

In more complex systems, with multiple converters connected to different grid nodes, choosing the most appropriate point for applying the aboveexplained method is not straightforward. To analyze stability properties of such systems, it is often beneficial to apply a different partitioning strategy [7], [8], [9], [10], [11], [12], [13], [14], [15], [16] than the traditional partitioning described above to two subsystems at a single point [4], [6]. The term *partitioning*, in this article, refers to the process of determining which elements of the system are assigned to each of the two subsystems, as well as defining the inputs and outputs (currents and voltages) for each subsystem. Different partitioning strategies were employed to address various challenges related to small-signal stability assessment. To analyze the stability of complex dc distribution grids [7], as well as point-to-point [9] and multiterminal [8] HVdc systems, the partitioning that groups all actively controlled devices, i.e., the converters, into one subsystem, while keeping the rest of the passive grid in the other subsystem is used. For identifying the source and cause of instability, partitioning based on the converters' physical location was utilized for participation factor analysis [10], [11], [12], [13], [14], [15]. This article, in addition to [16], exploits the use of appropriate partitioning, to derive decentralized impedance specifications in systems where converters are connected to multiple buses (nodes). The adopted partitioning involves grouping all converters, to which specifications are to be provided, into one subsystem while treating the rest of the grid as the other subsystem. This ensures that the structure of the minor loop gain is suitable for giving individual specifications to each converter.

Received 11 December 2024; revised 31 March 2025; accepted 14 May 2025. Date of publication 22 May 2025; date of current version 27 August 2025. This work was supported in part by the European Union's Horizon 2020 Research and Innovation Programme under the Marie Sklodowska-Curie Grant Agreement 101034319, in part by the European Union—NextGenerationEU, and in part by the project WIND-DIGIPOWER "Large-scale WIND integration for the future DIGItal POWER grid using innovative power electronics control and communication-based estimations" funded within the call "CETPartnership Joint Call 2022." Recommended for publication by Associate Editor G.-S. Seo. *(Corresponding author: Lazar Stojanović.)*

Lazar Stojanović and Paolo Mattavelli are with the Department of Management and Engineering, University of Padova, 36100 Vicenza, Italy (e-mail: lazar.stojanovic@phd.unipd.it; paolo.mattavelli@unipd.it).

Ružica Cvetanović and Simone Buso are with the Department of Information Engineering, University of Padova, 35131 Padova, Italy (e-mail: ruzica.cvetanovic@phd.unipd.it; simone.buso@dei.unipd.it).

Color versions of one or more figures in this article are available at https://doi.org/10.1109/TPEL.2025.3572309.

Digital Object Identifier 10.1109/TPEL.2025.3572309

Furthermore, inputs and outputs of these subsystems (voltages and currents) are chosen, so that no right half-plane (RHP) poles are present in the minor loop gain. These facts are crucial in the process of defining decentralized specifications.

While most of the aforementioned papers focus on analyzing the stability of complex systems with multiple converters, this article goes a step further by focusing on decentralized impedance specifications. Instead of solely assessing stability, these specifications establish a set of individual conditions that each converter's immittance must satisfy. By meeting these conditions, overall system stability is ensured. The ability to provide individual impedance specifications (decentralized specifications) to the converters connecting to the grid is advantageous in complex multivendor systems. For converter designers, specifications could serve as guidelines when designing converters, while for system operators, specifications could serve as a tool to ensure overall system stability.

The idea of decentralized impedance specifications was initially developed for multiple converters connected to a single dc bus [17], [18], [19]. To derive the specifications in [17], the forbidden region principle was applied. This principle restricts the Nyquist plot from entering a defined forbidden region, ensuring that the point $(-1, 0)$ is not encircled. In this way, stability is guaranteed if there are no RHP poles in the minor loop gain, which can be avoided if the system is partitioned properly. After the forbidden region is defined for the entire system, the decentralized specifications are defined in [17] by splitting the forbidden region among the converters, so each converter has its own condition that it must satisfy. Recently, the principle was extended to the case with a single ac bus [20].

All of the solutions mentioned above involve providing specifications for parallel converters connected to a single bus. The solution for imposing decentralized specifications for converters connected to different nodes of the ac grid was recently presented in [16]. This solution uses the abovementioned partitioning, where one of the subsystems contains all the converters, while the other contains the remaining grid's passive elements. Then, a combination of the small-phase and small-gain theorems is used to establish decentralized specifications, referred to as "decentralized conditions" in [16]. Although applying the small-gain theorem is straightforward, it is well known that it can lead to conservative results [21]. Therefore, combining it with the small-phase theorem helps to reduce this conservativeness [21]. However, applying the small-phase theorem requires the subsystems' immittance matrices to be sectorial and involves calculating the principal angles, a process that is not straightforward and potentially computationally intensive [22].

This article, for the first time, applies the Gershgorin theorem to impose decentralized specifications in multinode system. The applicability of the Gerhgorin theorem to the loop gain is ensured by using the appropriate partitioning strategy. To illustrate core principles without introducing unnecessary complexity, dc grid is considered, where each converter's immittance at its point of connection is simply a transfer function, rather than a transfer function matrix. However, the presented methodology can also be extended to ac grids, which will be addressed in future work.

Applying the Gershgorin theorem can lead to conservative results, especially around poorly damped resonances. To address this problem, this article proposes a combination of the specifications defined using the Gershgorin theorem with those defined based on the passivity theorem [4], [23].

The proposed decentralized specifications are computationally efficient and straightforward, reducing to an expression in the frequency domain that involves only simple complex number arithmetic. This makes the method applicable to large-scale systems. Additionally, it remains effective even when only black-box immittance measurements are available, making it particularly useful when converter parameters are unknown or not provided by the manufacturer.

The main novel contributions of this article are summarized as follows:

1) A particular partitioning of the system is applied, grouping the converters for which the specifications are to be given into a single subsystem. This ensures that the minor loop gain structure is well-suited for deriving decentralized specifications. Furthermore, inputs and outputs of the individual subsystems are chosen in a way that avoids RHP poles in the minor loop gain.
2) The individual conditions for each converter that guarantee the stability of the whole system—decentralized specifications—are developed by utilizing the Gershgorin theorem.
3) The conservativeness of imposing the specifications by only using the Gershgorin theorem is reduced by introducing a framework for combining different specifications. As one example that solves the conservativeness around poorly damped resonances, the Gershgorin theorem is combined with the passivity theorem. Resulting specifications are simple expressions in the frequency domain, making them computationally efficient and scalable to large-scale systems.
4) Application of the proposed specifications is illustrated based on both analytical impedance models of the converter, as well as on black-box measurements obtained from experimental results. It is experimentally demonstrated how violating specifications can lead to unstable oscillations, while compliance with the specifications ensures stable operation.

The rest of this article is organized as follows. Section II summarizes the impedance-based stability assessment and the forbidden region principle and presents the system partitioning that is suitable for defining decentralized specifications. Section III defines a general concept of decentralized specifications and proposes a new method to impose them based on the Gershgorin theorem. In addition, it presents a combination of the Gershgorin theorem and the passivity-based approach. Section IV exemplifies the use of the proposed methodology, providing a case study of three buck converters connected to different nodes of a dc grid. The proposed method is successfully applied with both analytical modeling of immittances and experimental black-box frequency response measurements. Finally, Section V concludes this article.

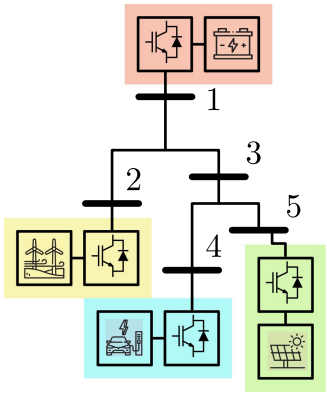

Fig. 1. Example of the distribution grid with multiple nodes.

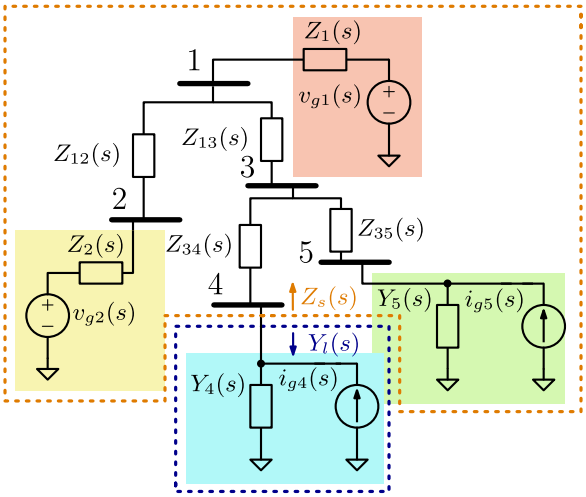

Fig. 2. Small signal impedance representation of distribution system in Fig. 1.

II. Impedance-Based Stability Assessment

A. Equivalent System Representation

To illustrate the method proposed in the article, an example is given in Fig. 1, which shows a simple dc grid with 5 nodes. Energy storage is connected on node 1, wind and solar sources are connected on nodes 2 and 5, and load represented with an electric vehicle charger is connected on node 4. Each node is connected to the dc grid through a PEC.

To apply the impedance-based approach, the system is represented as shown in Fig. 2. The converters connected to the grid are modeled using either Norton or Thevenin equivalents. In this representation, $i_{gk}(s)$ and $v_{gk}(s)$ are equivalent Norton and Thevenin generators at node k, respectively, while $Y_k(s)$ and $Z_k(s)$ are equivalent admittance and impedance.

Based on the converter topology and control implemented, converters are usually designed to be supplied from either an ideal current or a voltage source [24]. Due to this fact, the converters are classified as Z and Y-type [24], also referred to as voltage and current source in [6], respectively. Z-type converters are stable when loaded by an ideal current source and, therefore, do not exhibit RHP poles in $Z_k(s)$, although they may have RHP

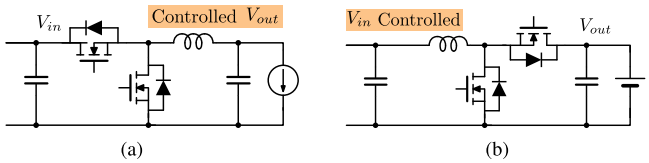

Fig. 3. Example of Y and Z-type converters. (a) Buck converter, loaded with constant current load, with output voltage control. (b) Boost converter, interconnecting the grid with the battery (connected to the output), with input voltage control. (a) Y-type converter. (b) Z-type converter.

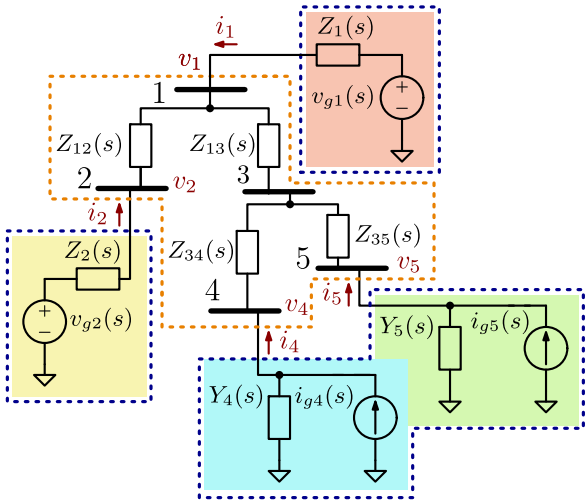

Fig. 4. Representation of partitioning the system from Fig. 2 at different nodes.

zeros. Similarly, Y-type converters are stable when supplied by an ideal voltage source and do not exhibit RHP poles in their admittance $Y_k(s)$ [24]. Due to the fact that Z-type converters are stable when supplied with an ideal current source, it is more natural to represent them as Thevenin equivalents. The same reasoning is applied for Y-type converters and the Norton representation [24]. An example of a Y-type converter is a buck converter whose output voltage is controlled, as shown in Fig. 3. This is because this converter is designed to be stable when supplied with a constant voltage source. On the other hand, an example of a Z-type converter is a boost converter whose input voltage is controlled, as shown in Fig. 3. This converter is designed to be stable when supplied with a constant current source, and will not operate properly when supplied with an ideal voltage source. Note that it is possible to design a converter that remains stable when supplied by both an ideal current and an ideal voltage source. In such a case, the converter can be represented using either a Norton or Thevenin equivalent model and will have no RHP poles in both its impedance and admittance.

In the example from Figs. 1, 2, 4, it is assumed that converters on nodes 1 and 2 are Z-type while converters connected to nodes 4 and 5 are Y-type converters. Properly representing converters to prevent the occurrence of RHP poles in the minor loop gain—by appropriately classifying them as either Z- or Y-type—is crucial for deriving decentralized specifications.

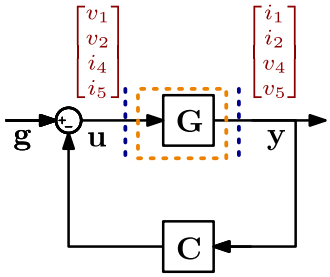

Fig. 5. Equivalent block diagram of partitioning from Fig. 4.

B. Stability Assessment At a Single Node

The most common way to apply the impedance-based stability assessment is to partition the system into two subsystems [4]. The system in Fig. 2, can be partitioned in multiple ways, where several converters would be part of one subsystem. For example, in Fig. 2 the system is partitioned at node 4, such that converter 4 is one subsystem with admittance $Y_l(s) = Y_4(s)$, while the rest of the system is aggregated as another subsystem with equivalent impedance $Z_s(s)$. Then the stability of the system can be assessed by applying the Nyquist criterion to minor loop gain $L(s) = Z_s(s)Y_l(s)$.

Although the stability of the system can be analyzed, this partitioning is not suitable for deriving decentralized specifications for two key reasons. First, the loop gain becomes a complex algebraic expression of the converters' impedances, making it challenging to impose individual specifications on each converter. Second, the resulting $L(s)$ may exhibit RHP poles due to the presence of multiple Z- and Y-type converter impedances/admittances in the equivalent impedance $Z_s(s)$. This characteristic prevents the application of the forbidden region principle [4], which is later used for the derivation of decentralized specifications.

C. Multinode Partitioning

To solve the problems outlined above, the system is partitioned as shown in Fig. 4. There, converters are grouped in one subsystem, and represented with proper Norton/Thevenin equivalents, while the grid is in the other subsystem. Then, the system can be represented with an equivalent feedback block diagram, Fig. 5, where $\mathbf{C}$ is the subsystem containing all the converter immittances, while $\mathbf{G}$ contains the rest of the grid. Grouping converters in one subsystem creates a convenient form for imposing individual specifications on them.

Another important thing is to select the inputs and outputs of the subsystems (voltages and currents in vectors $\mathbf{y}$ and $\mathbf{u}$) to avoid RHP poles in $\mathbf{C}(s)$, which is needed for the derivation of decentralized specifications. For a node where a Z-type converter is connected $\mathbf{y}$ is populated with the corresponding current i_k while vector $\mathbf{u}$ has the corresponding voltage v_k. While for a node with a Y-type converter, $\mathbf{y}$ and $\mathbf{u}$ are populated with v_k and i_k respectively. In this specific example, the vectors $\mathbf{y}$ and $\mathbf{u}$ are

$$\mathbf{y}(s) = \begin{bmatrix} i_1(s) & i_2(s) & v_4(s) & v_5(s) \end{bmatrix}^T$$

$$\mathbf{u}(s) = \begin{bmatrix} v_1(s) & v_2(s) & i_4(s) & i_5(s) \end{bmatrix}^T. \tag{1}$$

Then the matrix of converters' immittances $\mathbf{C}$ is

$$\mathbf{C}(s) = \begin{bmatrix} Z_1(s) & 0 & 0 & 0 \\ 0 & Z_2(s) & 0 & 0 \\ 0 & 0 & Y_4(s) & 0 \\ 0 & 0 & 0 & Y_5(s) \end{bmatrix}. \tag{2}$$

In Fig. 5, $\mathbf{G}(s)$ is the open-loop transfer function from $\mathbf{u}$ to $\mathbf{y}$ when converters are substituted with open circuits for Y-type, and short circuits for Z-type. Therefore, $\mathbf{G}(s)$ depends only on the grid structure and the impedances between nodes, $Z_{12}(s)$, $Z_{13}(s)$, $Z_{34}(s)$, $Z_{35}(s)$ in Fig. 4.

Current and voltages from ideal Thevenin and Norton generators are located inside $\mathbf{g}$ vector

$$\mathbf{g}(s) = \begin{bmatrix} v_{g1}(s) & v_{g2}(s) & i_{g4}(s) & i_{g5}(s) \end{bmatrix}^T. \tag{3}$$

The stability of the whole system can be judged by applying the generalized Nyquist criterion to the minor loop gain $\mathbf{L}(s) = \mathbf{C}(s)\mathbf{G}(s)$. The system is stable if there is no encirclement of the $(-1, 0)$ point by either eigenloci or $\det[\mathbf{I} + \mathbf{L}(s)] - 1$.

Depending on the application scenario, specifications can be imposed on all converters connected to the grid. In such cases, the $\mathbf{C}$ subsystem will contain all converters, while the grid subsystem, $\mathbf{G}$, will consist of only passive elements. Alternatively, when certain converters are inherently part of the grid and do not require imposing specifications, they can remain within the grid, as part of the $\mathbf{G}$ subsystem. The only constraint in this case is that the transfer function matrix $\mathbf{G}(s)$ does not have RHP poles.

D. Forbidden Region Principle

Once the minor loop gain is defined, it is of interest to define the forbidden region principle. This is later used to define decentralized specifications.

1) SISO Loop Gain: In the case where no RHP poles exist in minor loop gain $L(s)$ stability can be guaranteed by restricting the frequency response of loop gain $L(j\omega)$ from entering the forbidden region $\mathcal{F}$. The forbidden region $\mathcal{F}$ must be defined in such a way that if the minor loop gain frequency response, $L(j\omega)$, stays outside it, then no encirclement of $(-1, 0)$ is possible. With the forbidden region defined as such, the sufficient condition $\mathcal{S}$ for stability is

$$\mathcal{S} : \forall \omega \in \mathbb{R},\ L(j\omega) \notin \mathcal{F}. \tag{4}$$

2) MIMO Loop Gain: In the more general case, where the minor loop gain is a transfer function matrix $\mathbf{L}(s)$, which is the case in this article, the sufficient condition $\mathcal{S}$ for satisfying the forbidden region can be formulated by using eigenlocies or determinant

$$\mathcal{S} : \forall \omega \in \mathbb{R},\ \text{eig}[\mathbf{L}(j\omega)] \notin \mathcal{F} \vee \det[\mathbf{I} + \mathbf{L}(j\omega)] - 1 \notin \mathcal{F} \tag{5}$$

which guarantees stability according to the Generalized Nyquist criterion.

For example, one can define the forbidden region as everything left of the line that is parallel with the complex axis and

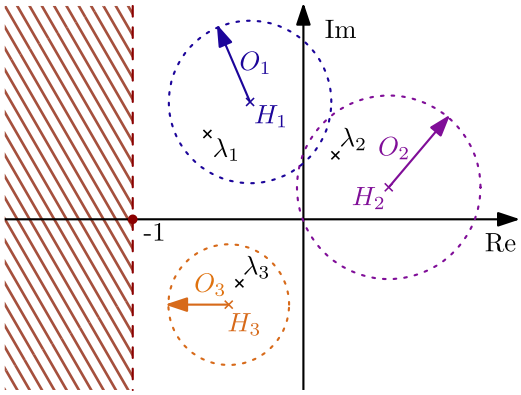

Fig. 6. Illustration of the Gershgorin theorem applied for loop gain with 3 converters, at a single frequency.

passes through the $(-1, 0)$ point, as represented by the red area of Fig. 6. Then, a sufficient condition for satisfying a forbidden region is

$$\mathcal{S}: \ \forall \omega \in \mathbb{R}, \ \mathrm{Re}\{\mathrm{eig}[\mathbf{L}(j\omega)]\} > -1. \tag{6}$$

III. Decentralized Specifications

A. Formulation of Decentralized Specifications

The main idea of decentralized specifications is to give individual specifications for each converter in such a way that they are not dependent on the other converter's immittances. Consider matrix $\mathbf{C}$ populated with Z and Y-type converters, with n being the total number of converters. The diagonal element of $\mathbf{C}$ matrix is $C_k(s) = \mathbf{C}(k,k)(s)$, which is either impedance or admittance depending on the converter type. Then the decentralized specifications are given as n individual conditions $\mathcal{Q}_1, \ldots, \mathcal{Q}_k, \ldots, \mathcal{Q}_n$, where each condition is only dependent on one converter immittance $C_k(s)$ and $\mathbf{G}(s)$. In the frequency domain, each condition is given in a form

$$\mathcal{Q}_k : \forall \omega, \ f_k\left(C_k(j\omega), \mathbf{G}(j\omega)\right) > M_k. \tag{7}$$

In order for decentralized specification to guarantee stability, f_k and M_k must be selected such that, if all conditions are met, the stability of the system is ensured. The possible methods for selecting f_k and M_k will be discussed in the following subsections.

Assume that the sufficient condition for stability of the interconnected system, like one in Fig. 2, is $\mathcal{S}$, then our goal is to provide a set of conditions $\mathcal{Q}_k$, $\{k \in \mathbb{N} | \ 1 \leq k \leq n\}$ in such a way that satisfying each condition $\mathcal{Q}_k$ is sufficient for system stability

$$\mathcal{Q}_1 \wedge \cdots \wedge \mathcal{Q}_k \wedge \cdots \wedge \mathcal{Q}_n \rightarrow \mathcal{S}, \ 1 \leq k \leq n. \tag{8}$$

It is important to note that decentralized specifications are not merely used for judging the stability of the system, but also for providing specifications for individual converters' immittance. When applying stability criteria—such as the Generalized Nyquist criterion to the minor loop gain—the immittances of all converters must be known. On the other hand, by establishing specifications for each converter, the stability of the system can be ensured as long as these specifications are met. This approach provides converter designers with clear requirements that they must satisfy in order to guarantee stability.

Moreover, the proposed approach is particularly useful when integrating converters from multiple vendors, as the designer of one converter does not need to know the parameters of other converters—only the specifications assigned to his or her own. Additionally, it allows converter providers to keep their parameters confidential, as compliance with the given specifications guarantees system stability.

Along this line, subsequent subsections discuss newly proposed decentralized specifications based on the Gershgorin theorem and their combination with a passivity-based approach.

B. Decentralized Specifications Based on Gershgorin Theorem

To solve the problem of defining the decentralized specifications for the case where converters are connected to multiple nodes in the grid, like in Fig. 4, the partitioning mentioned in Section II-C will be used.

The minor loop gain of the whole system with n converters is $\mathbf{L}(s) = \mathbf{C}(s)\mathbf{G}(s)$ or in matrix form

$$\begin{aligned}\mathbf{L} &= \begin{bmatrix} C_1 & 0 & \cdots & 0 \\ 0 & C_2 & \cdots & 0 \\ \vdots & \vdots & \ddots & \vdots \\ 0 & 0 & \cdots & C_n \end{bmatrix} \cdot \begin{bmatrix} G_{11} & G_{12} & \cdots & G_{1n} \\ G_{21} & G_{22} & \cdots & G_{2n} \\ \vdots & \vdots & \ddots & \vdots \\ G_{n1} & G_{n2} & \cdots & G_{nn} \end{bmatrix} \\ &= \begin{bmatrix} C_1G_{11} & C_1G_{12} & \cdots & C_1G_{1n} \\ C_2G_{21} & C_2G_{22} & \cdots & C_2G_{2n} \\ \vdots & \vdots & \ddots & \vdots \\ C_nG_{n1} & C_nG_{n2} & \cdots & C_nG_{nn} \end{bmatrix}\end{aligned} \tag{9}$$

where "(s)" is omitted for more compact writing. The final expression for loop gain has a property that each row is only dependent on one converter immittance $C_k(s)$. To use this property for defining the decentralized specifications, we need to recall the Gershgorin circle theorem first.

The Gershgorin theorem [25] states that if A is a complex square matrix with the order of n

$$A = \begin{bmatrix} a_{11} & \cdots & a_{1n} \\ \vdots & \ddots & \vdots \\ a_{n1} & \cdots & a_{nn} \end{bmatrix} \tag{10}$$

then the eigenvalues of A must lie in n circles on the complex plane. The center of each circle is located in a_{kk}, while the radius of the corresponding circle is $\sum_{i \neq k} |a_{ki}|$.

Since the frequency response of minor loop gain $\mathbf{L}(j\omega)$ is a matrix of complex numbers at each frequency, the Gershgorin theorem can be applied.

For example, if we take the system with 3 converters, then at single frequency ω_c the response is a complex matrix

$$\mathbf{L}(j\omega_c) = \begin{bmatrix} \underline{C_1}\underline{G_{11}} & \underline{C_1}\underline{G_{12}} & \underline{C_1}\underline{G_{13}} \\ \underline{C_2}\underline{G_{21}} & \underline{C_2}\underline{G_{22}} & \underline{C_2}\underline{G_{23}} \\ \underline{C_3}\underline{G_{31}} & \underline{C_3}\underline{G_{32}} & \underline{C_3}\underline{G_{33}} \end{bmatrix} \tag{11}$$

where underlined values represent the response at single frequency $\underline{C_1} = C_1(j\omega_c)$. According to the Gershgorin theorem the eigenvalues of $\mathbf{L}(j\omega_c)$, $\lambda_{1,2,3}(j\omega_c)$, must lay inside 3 circles with center $H_k = \underline{C_k}\underline{G_{kk}}$, and radius O_k being the sum of the absolute value of nondiagonal elements of the same row

$$\begin{aligned} H_1 &= \underline{C_1}\underline{G_{11}}, O_1 = |\underline{C_1}\underline{G_{12}}| + |\underline{C_1}\underline{G_{13}}| \\ H_2 &= \underline{C_2}\underline{G_{22}}, O_2 = |\underline{C_2}\underline{G_{21}}| + |\underline{C_1}\underline{G_{23}}| \\ H_3 &= \underline{C_3}\underline{G_{33}}, O_3 = |\underline{C_3}\underline{G_{31}}| + |\underline{C_3}\underline{G_{32}}|. \end{aligned} \tag{12}$$

Application of the Gershgorin theorem is illustrated in Fig. 6.

The sufficient condition for system stability is $\mathcal{S} : \forall\omega,\ \text{eig}[\mathbf{L}(j\omega)] \notin \mathcal{F}$. Thus, keeping all the circles outside the forbidden region for each frequency will guarantee stability according to the Gershgorin theorem. For example, if we assume a forbidden region such that the stability condition is

$$\mathcal{S} : \forall\omega,\ \text{Re}\{\text{eig}[\mathbf{L}(j\omega)]\} > -1 \tag{13}$$

then applying the Gershgorin theorem will yield n separate conditions

$$\mathcal{Q}_k : \text{Re}\{C_k(j\omega)G_{kk}(j\omega) + \sum_{i=1|i\neq k}^{n} |C_k(j\omega)G_{ik}(j\omega)|\} > -1. \tag{14}$$

These conditions, which are sufficient for stability, are only dependent on a single converter's immittance (C_k). This makes conditions suitable for imposing the decentralized specifications. The Gershgorin theorem allowed us to find the suitable condition $\mathcal{Q}_k$ from (7), such that the stability of the system is guaranteed if all conditions are satisfied.

C. Different Forbidden Regions

Forbidden region from (13) is easy to implement. However, it introduces conservativeness since it restricts the eigenloci from entering a significant region in a complex plane. To make specifications less conservative, the area of the forbidden region can be minimized, and it can be defined as a half-line that is part of the real axis from $(-1, 0)$ to $(-\infty, 0)$, as shown in Fig. 7. If there is no intersection of Gershgorin circles with this half-line, there is no crossing of the real axis to the left of $(-1, 0)$. This implies no encirclements of $(-1, 0)$ and, thus, a stable system.

To implement this forbidden region in the form of specifications, we first define the parameter D for each converter. The parameter D has the property that it is greater than zero when there is no intersection between the forbidden region and the circle. In this case, D represents the minimal distance between the circle and the forbidden region, as shown in Fig. 7. In contrast, when $D < 0$, there is an intersection between the circle and the forbidden region, which means that the eigenloci *could*

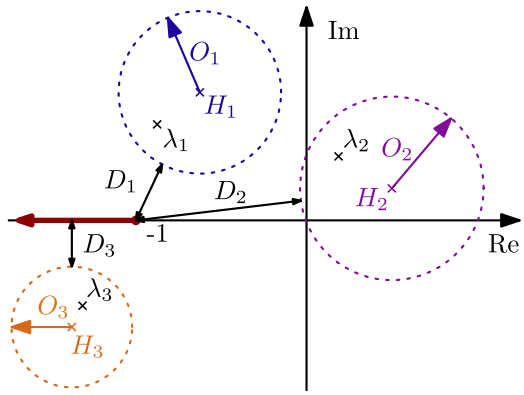

Fig. 7. Illustration of less conservative forbidden region.

encircle $(-1, 0)$

$$D_k(j\omega) = \begin{cases} |H_k(j\omega) + 1| - O_k(j\omega),\ \text{Re}\{H_k(j\omega)\} \geq -1 \\ |\,\text{Im}\{H_k(j\omega)\}| - O_k(j\omega),\ \text{Re}\{H_k(j\omega)\} < -1. \end{cases} \tag{15}$$

These properties of D enable us to define the decentralized specifications as

$$\mathcal{Q}_k : \forall\omega \in \mathbb{R},\ D_k(j\omega) > 0. \tag{16}$$

D. Specifications by Using Passivity Approach

Instead of looking at the Gershgorin circles and estimating the position of eigenvalues, another approach for defining the decentralized specifications is to apply the passivity concept [23]. The passivity concept is based on energy dissipation and states that the feedback interconnection of two passive systems results in a passive system as well. Passive systems are stable by definition [23]. Therefore, if both $\mathbf{C}$ and $\mathbf{G}$ are passive, the resulting system will also be passive and, consequently, stable. The connection between the passivity of the system with transfer function $\mathbf{C}(s)$ and frequency response $\mathbf{C}(j\omega)$ is stated in [23]. The system is passive if $\mathbf{C}(s)$ is stable and

$$\mathbf{C}(j\omega) + \mathbf{C}^H(j\omega) > 0 \tag{17}$$

where "H" indicates hermitian conjugate transpose.

If we assume that the grid ($\mathbf{G}$) is passive, due to the structure of the $\mathbf{C}$ matrix, the sufficient conditions $\mathcal{P}_k$ for system stability are

$$\mathcal{P}_k : \forall\omega \in \mathbb{R},\ \text{Re}\{C_k(j\omega)\} > 0. \tag{18}$$

These conditions are only dependent on one converter at a time, which means they are in the form of decentralized specifications.

E. Combination of Different Ways for Imposing Decentralized Specifications

Imposing decentralized specifications with a passivity approach, as in Section III-D, is simple. Nevertheless, it requires the converters to be passive, i.e., dissipate the energy at all frequencies. This is not possible due to the desired power conversion and regulation capabilities, as well as the system delays. On

the other hand, the method relying on the Gershgorin theorem, presented in Sections III-B and III-C, exhibits conservativeness related to circles being the possible locations of eigenvalues. Since the radius of circles is dependent on absolute values of terms (12), having poorly damped resonances can potentially lead to very conservative specifications.

A similar combination of conditions was used to reduce the conservativeness of the small-gain theorem by combining it with the small-phase theorem [16], [21]. To make the aggregated condition for stability, we need to define the conditions as dependent on frequency, $\mathcal{Q}_k(\omega)$, $\mathcal{P}_k(\omega)$. Now we can define the sufficient condition for system stability $\mathcal{S}$, by using (15), (16), and (18), as

$$\left\{\forall\omega,\ \underbrace{[\mathcal{Q}_1(\omega)\wedge\ldots\wedge\mathcal{Q}_n(\omega)]}_{\text{Gershgorin specs. } D_k(j\omega)>0}\vee\underbrace{[\mathcal{P}_1(\omega)\wedge\ldots\wedge\mathcal{P}_n(\omega)]}_{\text{Passivity Re}\{C_k(j\omega)\}>0}\right\}\rightarrow\mathcal{S}. \tag{19}$$

This means that the system is stable if for every frequency either all converters satisfy the Gershgorin specifications or all converters are passive. Proof of this theorem is given in the Appendix.

Note that the combination of specifications based on the Gershgorin theorem and the passivity is not the only possible option, and other combinations are theoretically possible. Intuitively, the Gershgorin theorem is conservative around resonances, as its cross-coupling terms are based on immittance magnitudes. To overcome this, it is natural to use another method that is nondependent on the immittance magnitudes. One example of such a method is the passivity theorem. However, it is not possible to rely solely on passivity since converters are usually not passive in the low frequency range due to the control requirements. Therefore, combining these two specifications appears to be a natural choice for reducing conservativeness. Further analysis and comparisons of different combinations are left for future work.

IV. Application Scenario

A. System Description and Modeling

To test the proposed method, we consider an example scenario consisting of three buck converters connected to a voltage source through nonideal cables, as shown in Fig. 8. The control of the buck converters is designed with the inner current and the outer voltage loop. The converter controllers are implemented digitally. The control execution frequency is twice the switching frequency, and the reference is updated twice per switching period. Current i_L is oversampled with an oversampling factor of 16 and then filtered with a moving average filter having a window equal to one switching period to remove feedback acquisition noise. The parameters of the system considered are given in Table I.

To analytically model the grid, we use the cable lumped parameter model, as shown in Fig. 9. Because the output voltage of buck converters is controlled, they behave as Y-type converters, and the Norton equivalent is used for their representation, as elaborated in Section II-A.

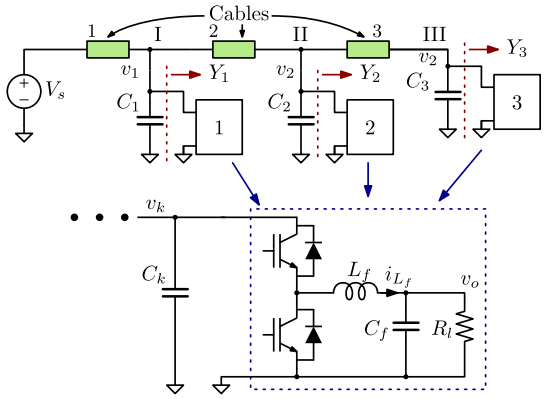

Fig. 8. Test case scenario of 3 buck converters connected to a dc grid.

TABLE I
Parameters of the Considered System

Cable parameters	**Cab. 1**	**Cab. 2**	**Cab. 3**
Parasitic cable inductance L	360 µH	390 µH	390 µH
Parasitic cable resistance R	40 mΩ	40 mΩ	40 mΩ
Converters parameters	**Cnv. 1**	**Cnv. 2**	**Cnv. 3**
Buck converters input capacitance C	240 µF	240 µF	240 µF
Output buck voltage V_o	24 V	24 V	24 V
Filter inductance L_f	180 µH	360 µH	720 µH
Filter capacitance C_f	1.3 mF	1.7 mF	2.2 mF
Restive load R_l	2.2 Ω	2.2 Ω	2.2 Ω
Switching frequency f_{sw}	13 kHz	10 kHz	10 kHz
Sampling frequency f_s	26 kHz	20 kHz	20 kHz
Number of samples for averaging N *	16	16	16
Current control bandwidth	300 Hz	500 Hz	800 Hz
Current control bandwidth (changed)†	300 Hz	250 Hz	800 Hz
Voltage control bandwidth	50 Hz	80 Hz	150 Hz
Voltage control bandwidth (changed)†	50 Hz	40 Hz	150 Hz
Adding parallel RC damper‡	No	No	Yes

*Number of samples taken per switching period. These samples are then averaged to obtain signals without switching ripple.
†Parameters of controllers are changed to satisfy the violated specifications.
‡Parallel RC damper added to satisfy specifications $R_d = 2.2\,\Omega$, $C_d = 1.3\,\text{mF}$.

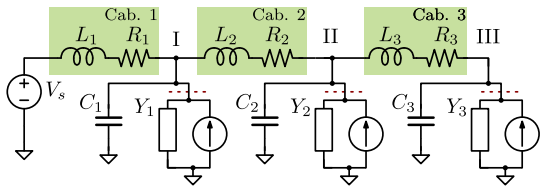

Fig. 9. Small signal impedance representation of the system in Fig. 8.

To obtain the converters' admittance model, small-signal s-domain average representation of the converter and its control loop is given in Fig. 10. The voltage and current PI controllers are labeled as $K_v(s)$ and $K_i(s)$, respectively. The transfer function from the duty cycle d to the output voltage v_i, $G_p(s)$, represents PWM modulator model involving double update strategy [26].

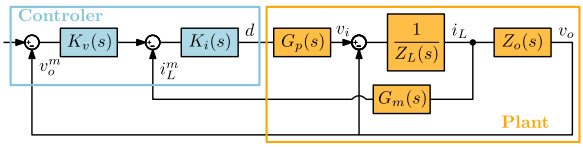

Fig. 10. Control diagram of the buck converters.

Finally, $G_m(s)$ is the transfer function from i_L to the filtered inductor current i_L^m, and it represents the moving average filter used for current feedback. It is modeled as a simple delay of half the switching period T_{sw}.

The impedance of the inductor L_f is $Z_L(s) = sL_f + R_{L_f}$ and the impedance of the capacitor C_f is $Z_C(s) = \frac{1}{sC_f}$. The parallel impedance of the output capacitor and the load is $Z_o(s) = (\frac{1}{sC_f} + R_{C_f})||R_l$.

In the end, the analytical expression for the buck converter input admittance is

$$Y(s) = \frac{D^2 - I_{in}K_iG_pG_m(1 - K_vZ_o)}{Z_L + Z_o + V_{in}K_iG_pG_m(1 + K_vZ_o)}. \tag{20}$$

Writing the "(s)" was omitted for the sake of simplicity.

B. System Partitioning

By applying the partitioning, discussed in Section II-C, to the representation in Fig. 9, the matrix $\mathbf{C}$ is populated with buck converters' input admittances

$$\mathbf{C}(s) = \begin{bmatrix} Y_1(s) & 0 & 0 \\ 0 & Y_2(s) & 0 \\ 0 & 0 & Y_3(s) \end{bmatrix}. \tag{21}$$

From the circuit in Fig. 9, we can derive the $\mathbf{G}(s)$ matrix as a transfer function from the input voltages to the input currents of the buck converters

$$\mathbf{G}(s) = \begin{bmatrix} G_{11}(s) & G_{12}(s) & G_{13}(s) \\ G_{21}(s) & G_{22}(s) & G_{23}(s) \\ G_{31}(s) & G_{32}(s) & G_{33}(s) \end{bmatrix}. \tag{22}$$

Applied partitioning ensures that there are no RHP poles in the minor loop gain $\mathbf{L}(s) = \mathbf{C}(s)\mathbf{G}(s)$. This is true because $\mathbf{G}(s)$ has no RHP poles nor zeros, while $\mathbf{C}(s)$ contains only RHP zeros.

C. Stability Assessment Using the Generalized Nyquist Criterion

To analyze the stability of the system, the Generalized Nyquist criterion is applied to the minor loop gain $\mathbf{L}(s) = \mathbf{C}(s)\mathbf{G}(s)$. Since $\mathbf{L}(s)$ has no RHP poles, the system is stable if there is no encirclement of $(-1, 0)$ point by eigenloci $(\lambda_{1,2,3}(j\omega))$. From the Nyquist plot in Fig. 11, we can conclude that the system is unstable, since $\lambda_3(j\omega)$ encircles the $(-1, 0)$ point. Applying the Generalized Nyquist criterion gives information about system stability, but the downside is that it does not give information about the cause of the instability. Moreover, the

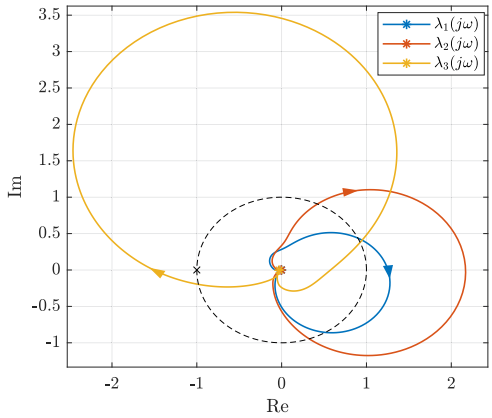

Fig. 11. Generalized Nyquist plot of the minor loop gain $\mathbf{L}(j\omega)$ eigenlocies $\lambda_{1,2,3}(j\omega)$, when $\omega \in (0, \infty)$, "*" marker represents the starting point of the curve ($\omega = 0$).

Generalized Nyquist Criterion can only be applied to a whole system and does not provide specific guidance for designing individual controllers to prevent instability. These facts make it difficult to apply the Generalized Nyquist Criterion in the case when converters are originating from different vendors, and not all their impedances are known upfront.

D. Applying Proposed Decentralized Specifications

Proposed decentralized specifications, defined by the combination of Gershgorin theorem and passivity (19), address exactly these challenges. To define the decentralized specifications we first identify the frequency regions for the satisfaction of the Gershorin theorem and passivity. Because buck converters have output voltage controlled, they cannot be passive in low frequency range. Furthermore, the delay present in the digital control implementation can cause the admittance to be nonpassive at high frequencies. Therefore, in this example, we consider that converters should be passive in the frequency range from 140 Hz to 2 kHz. The specifications based on the Gershgorin theorem are used to guarantee the stability for the low (less than 140 Hz) and high (more than 2 kHz) frequency ranges. The selection of frequency ranges is based on the specific system parameters and must be determined individually for each system. In this case, multiple resonant frequencies are present in the grid within the 140 Hz to 2 kHz range. As a result, the Gershgorin-based specifications, which depend on immittance magnitudes, are likely to be violated. Therefore, ensuring the passivity of the converter in this frequency region is needed, as discussed in Section III-E.

Proposed decentralized specifications for each converter are given in Fig. 12. For the converter 1 Fig. 12(a), the Gershgorin part of the specifications $(D_1(j\omega))$ is violated in the frequency range around 200 and 700 Hz, but satisfied in required region low (less than 140 Hz) and high (more than 2 kHz) frequency region. Since converter 1 is passive in frequency region from 140 Hz to 2 kHz, converter 1 satisfies specifications.

The converters 2 and 3 are not satisfying the specifications, as shown in Fig. 12(b) and (c). This is because they are

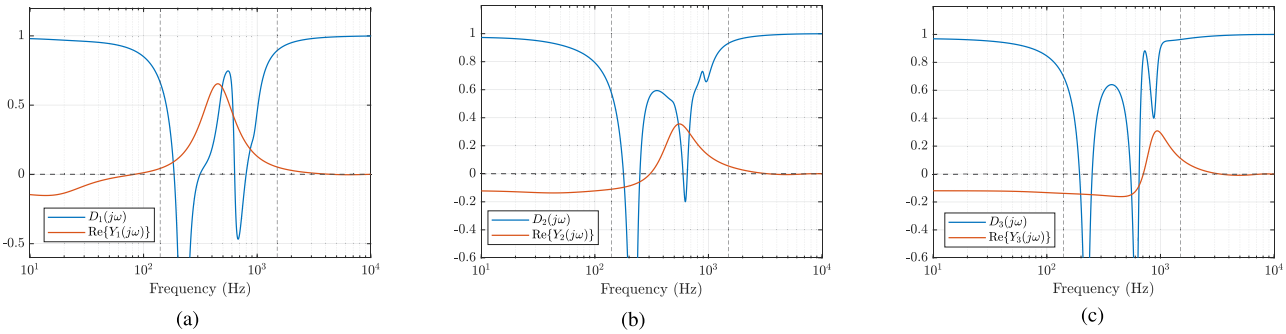

Fig. 12. Proposed decentralized specifications evaluation for each converter connected to the grid. (a) Converter 1. (b) Converter 2. (c) Converter 3.

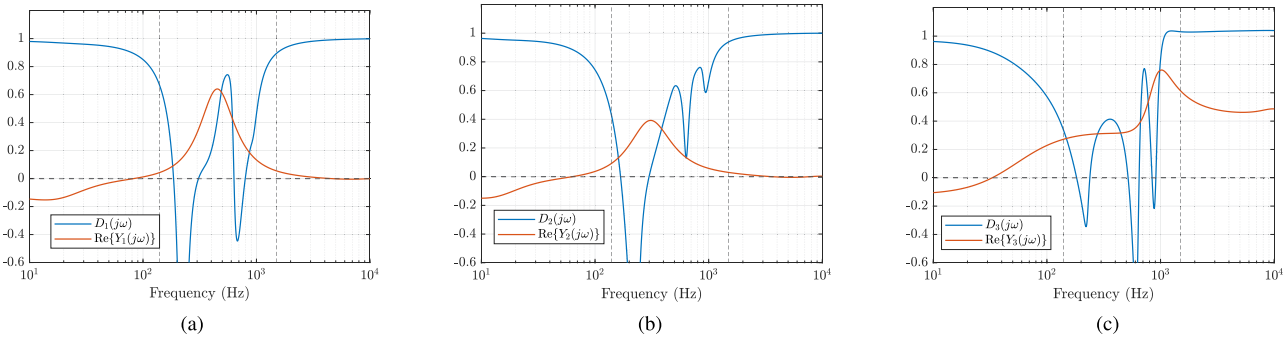

Fig. 13. Proposed decentralized specifications evaluation for each converter connected to the grid with changed converter 2 & 3 control parameters. (a) Converter 1 (unchanged). (b) Converter 2 (lowered bandwidth). (c) Converter 3 (added *RC* damper).

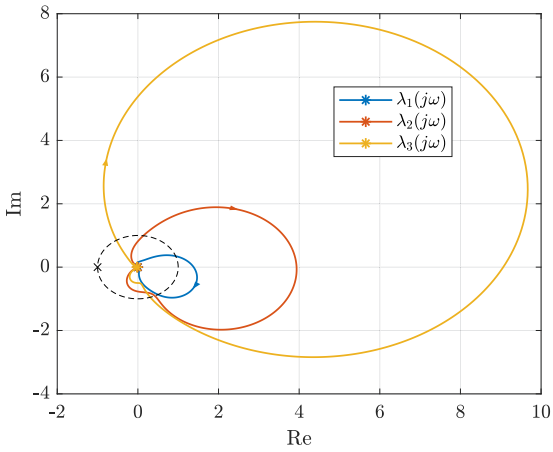

Fig. 14. Generalized Nyquist plot of the minor loop gain $\mathbf{L}(j\omega)$ eigenlocies $\lambda_{1,2,3}(j\omega)$, when $\omega \in (0, \infty)$, with changed control parameters. Marker "*" represents the starting point of the curve ($\omega = 0$).

not passive in the frequency range from 140 Hz to 2 kHz, where $D_{1,2,3}(j\omega) < 0$. According to the proposed decentralized specifications, passivizing the converters 2 and 3 in the frequency range from 140 Hz to 2 kHz will stabilize the system (19).

Note that the specifications are provided to each converter separately, and each converter designer can apply the specifications without knowing the other converters' impedances. In practice, converters 2 and 3 would not be eligible for connection

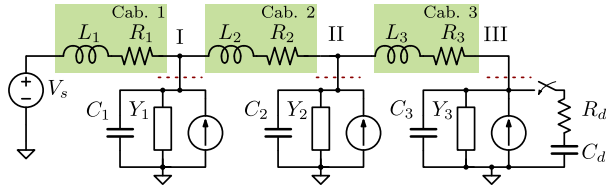

Fig. 15. Test case scenario when input capacitors are considered as a part of the converter.

since they do not satisfy the specifications. The particular order of presenting results in the article, where we first present an unstable system and then make the converter satisfy the specifications, was done to better illustrate the motivation and implications of the proposed method. In practice, the specifications would be applied before connecting the converters, thus guaranteeing the stability of the system.

E. Stabilizing the System

To stabilize the system, we can change the parameters of converters 2 and 3 to make them passive in the frequency range from 140 Hz to 2 kHz. For converter 2, we lower the bandwidth of the current and voltage control loops to 250 and 40 Hz, respectively. If we assume that lowering the bandwidth for converter 3 is not acceptable, alternatively, we can add a parallel RC damper ($C_d = 1.3\text{mF}$ $R_d = 2.2\Omega$) to the converter

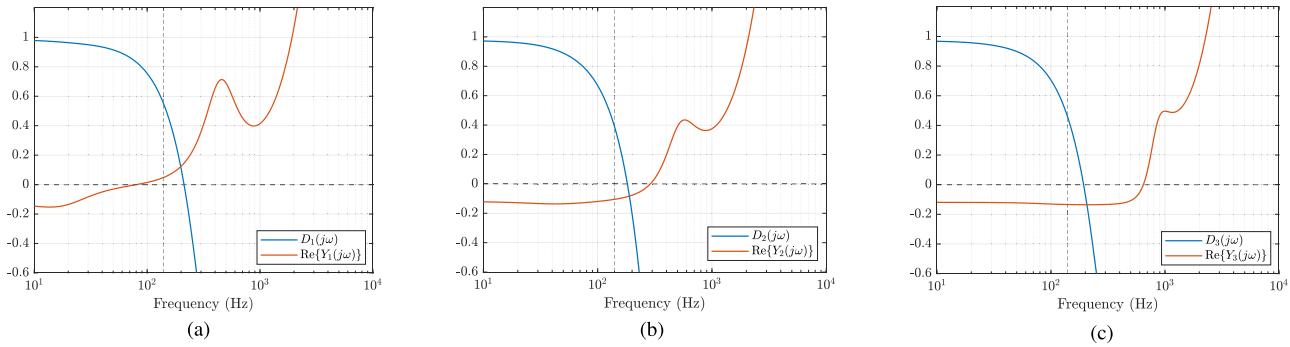

Fig. 16. Proposed decentralized specifications evaluation when input capacitors are considered as a part of the converter. (a) Converter 1. (b) Converter 2. (c) Converter 3.

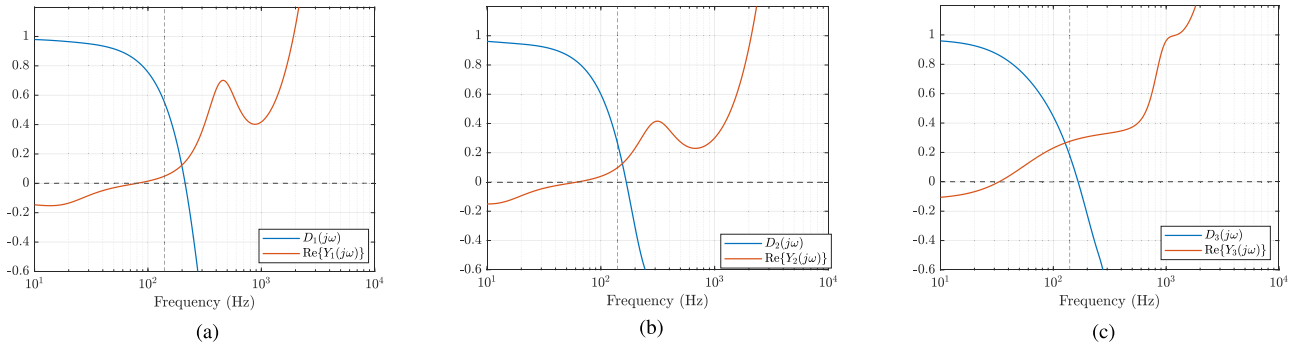

Fig. 17. Proposed decentralized specifications evaluation when input capacitors are considered as a part of the converter, with changed converter 2 & 3 parameters. (a) Converter 1 (unchanged). (b) Converter 2 (lowered bandwidth). (c) Converter 3 (added *RC* damper).

3 input. This change ensures that both converters 2 and 3 become passive in the required frequency range, as shown in Fig. 13, and thus satisfy the proposed specifications. From the Nyquist plot in Fig. 14, we can observe that the system is stable, which is expected since satisfying the decentralized specifications is a sufficient condition for stability.

F. Partitioning Converter Input Filter

During the previous analysis, we assumed that the input capacitors of the converters are part of the grid. With this approach, the grid contains several resonances, and usually, stability problems occur around those resonances, which makes identifying the problem easier and more intuitive.

However, in practice, the input capacitor is usually integrated as a part of the converter, Fig. 15, due to the converter's switching nature. Although it is possible to analytically derive the converter admittance without the input capacitor, measuring this admittance is not practical. Since these proposed decentralized specifications can be applied only by knowing the black box frequency responses of the converter and the grid, it is important to consider the input capacitor as part of the converter.

Since now the capacitor is considered part of the converter, the passivity of the converter and the capacitor is guaranteed at high frequencies due to the capacitor series resistance. So, in this consideration, specifications are divided into two sections: low frequency (less than 140 Hz), where converters should satisfy the Gershgorin theorem, and high frequency (higher than 140 Hz), where converters should be passive. The application of the decentralized specifications when the input capacitor is considered part of the converter is given in Figs. 16 and 17.

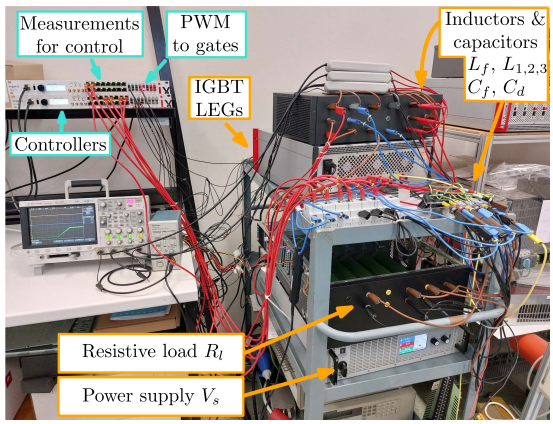

Fig. 18. Laboratory setup used for testing.

For the results in Fig. 16, the system is the same one represented in Fig. 12, while input capacitors are considered part of the converter. From Fig. 16 we can conclude that the specifications are satisfied for converter 1, while converters 2 and 3 do not satisfy the specifications, since converters are not fully passive above 140 Hz.

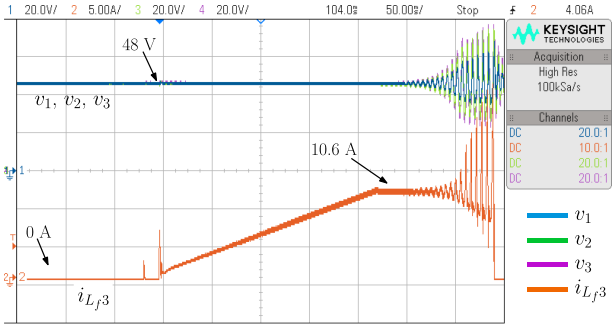

(a)

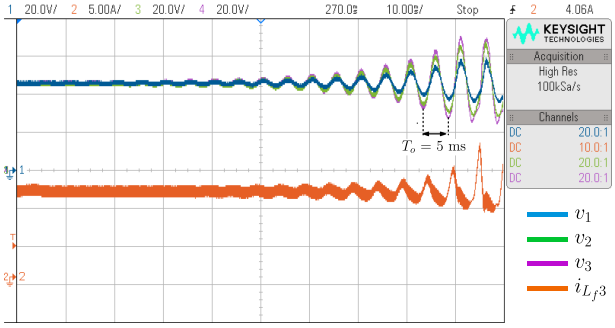

(b)

Fig. 19. Instability occurring during the turn-ON of converter 3. (a) Full view. (b) Zoomed view of oscillations.

For the results in Fig. 17, the system is the same one represented in Fig. 13 and the specifications are satisfied for all converters. This was achieved by passivizing converters 2 and 3 in the frequency range above 140 Hz.

This shows that for the two scenarios analyzed, the same conclusions are drawn, independently of whether the capacitor is considered part of the converter or the grid.

G. Experimental Validation

To experimentally validate the proposed method, the system from Fig. 8 was implemented in the laboratory, as shown in Fig. 18, by using the Imperix rapid prototype system. The buck converters are implemented with PEB8032 modules, while the control is executed on two Imperix B-Boxes, such that one B-Box controls converter 1 while the other controls converters 2 and 3. The B-Box collects measurements of voltages and currents from the sensors and transmits the PWM signals to the gates of the PEB8032 modules via optical cables. The parameters of the system remain consistent with those discussed in previous sections and are summarized in Table I.

The experimental test was conducted in the following manner. First, the input voltage of the converters was initialized to 48 V, and the converters were turned ON one by one by gradually increasing the reference output voltage from 0 to 24 V. During the turning ON of converters 1 and 2, no instability was observed; however, during the turning ON of converter 3, instability was observed, as shown in Fig. 19. The period of the undamped oscillations T_o is 5 ms.

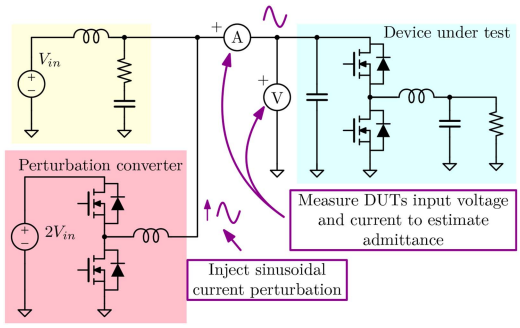

Fig. 20. Perturbation injection for measuring the converters' admittance.

The advantage of the proposed decentralized specifications is that they can be applied by using black-box immittance measurements of the converters and the grid, without the need for the analytical model. To illustrate this, the admittances $Y_k(j\omega)$ of the converters are measured as shown in Fig. 20. The converter (device under test DUT) is first connected to the nonideal voltage source, created by adding the damped LC filter to the dc power supply. This enables the perturbation of the input converters' (DUTs) voltage. Then, the sinusoidal perturbation of DUT input voltage is achieved by injecting the sinusoidal current from the perturbation converter. To minimize interactions between the DUT and the perturbation converter, the perturbation converter operates at a significantly higher switching frequency of 100 kHz. The DUT's admittance is obtained by measuring its input voltage and current, calculating the Fourier coefficients at the perturbation frequency, and subsequently determining the admittance as the ratio of the current and voltage Fourier coefficients. The Fourier coefficients are calculated as

$$\underline{I} = \frac{1}{N_p T_c} \int_0^{N_p T_c} i(t) e^{-j\omega_c t} dt \tag{23}$$

where N_p is the number of periods of perturbation signal, the period of the perturbation signal is $T_c = \frac{2\pi}{\omega_c}$, and $i(t)$ is time domain measurement of current or voltage. The measurements are done for the 40 points in the frequency range from 20 Hz to 2 kHz.

The grid immittance matrix $\mathbf{G}(j\omega)$ is measured in a similar manner by injecting a small current perturbation into each node I, II, and III using the perturbation converter, while the converters are physically disconnected from the grid. The voltage responses at the nodes $v_{1,2,3}$ are measured to obtain the grid's frequency response. To determine the frequency response of $\mathbf{G}$ at a single frequency ω_c, the perturbation current is injected at one node at a time, and the procedure is repeated for each node. This results in three independent measurements at ω_c. In the first measurement, the perturbation current $i_p^{m_1}$ is injected at node I, and the corresponding node voltages $v_1^{m_1}$, $v_2^{m_1}$, and $v_3^{m_1}$ are recorded. In the second measurement, the perturbation current $i_p^{m_2}$ is injected at node II, with the corresponding voltages $v_1^{m_2}$, $v_2^{m_2}$, and $v_3^{m_2}$ measured. The same procedure is applied for node III, completing the set of measurements.

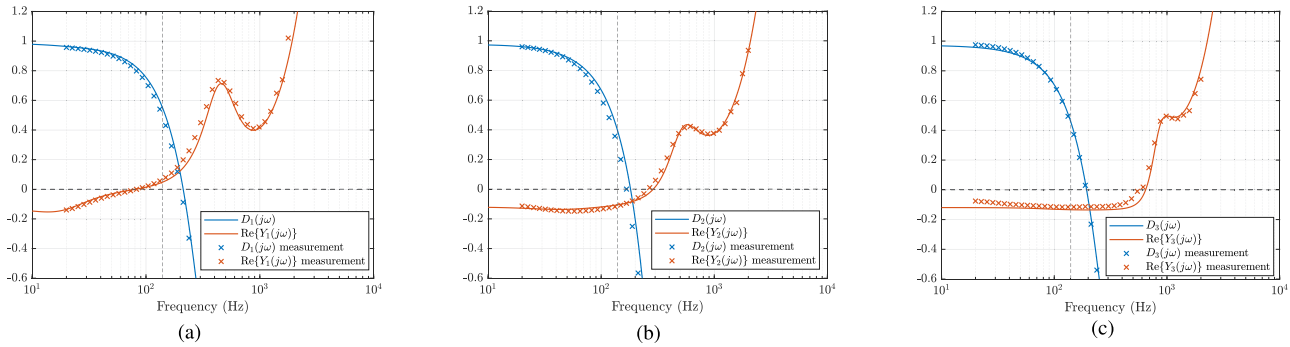

Fig. 21. Proposed decentralized specifications evaluation for measured values obtained from the experimental setup. (a) Converter 1. (b) Converter 2. (c) Converter 3.

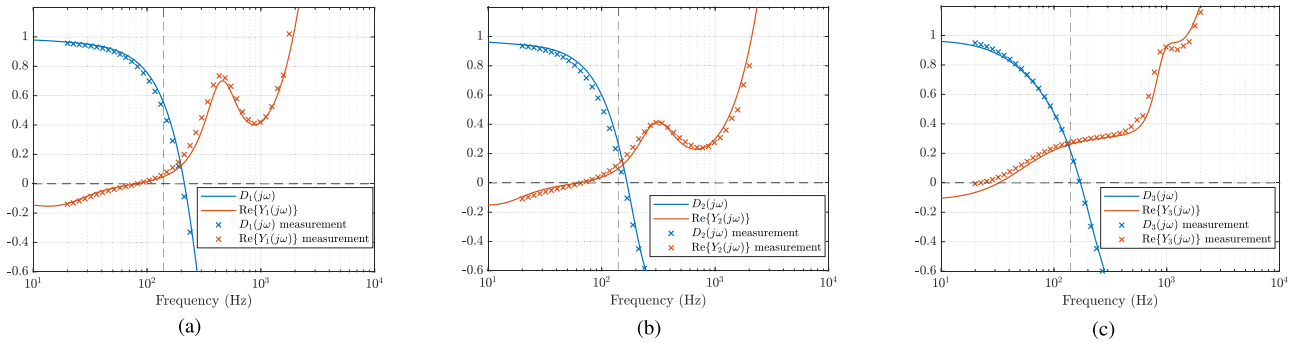

Fig. 22. Proposed decentralized specifications evaluation for each converter connected to the grid with changed converter 2 & 3 control parameters, experimental results. (a) Converter 1 (unchanged). (b) Converter 2 (lowered bandwidth). (c) Converter 3 (added *RC* damper).

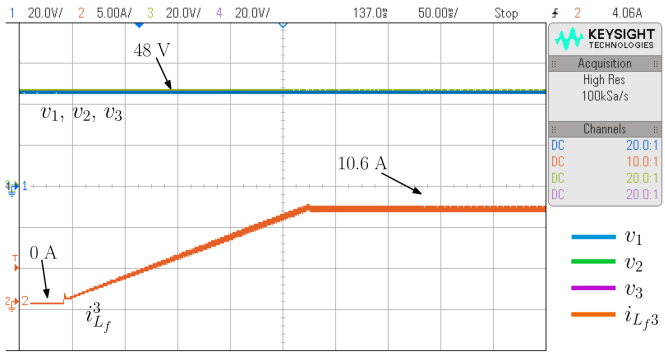

Fig. 23. Turning ON of the third converter, same as in Fig. 19, with satisfied specifications.

The $\mathbf{G}(j\omega_c)$ is then calculated as

$$\mathbf{G}(j\omega_c) = \begin{bmatrix} \underline{I}_p^{m_1} & 0 & 0 \\ 0 & \underline{I}_p^{m_2} & 0 \\ 0 & 0 & \underline{I}_p^{m_3} \end{bmatrix}^{-1} \begin{bmatrix} \underline{V}_1^{m_1} & \underline{V}_2^{m_1} & \underline{V}_3^{m_1} \\ \underline{V}_1^{m_2} & \underline{V}_2^{m_2} & \underline{V}_3^{m_2} \\ \underline{V}_1^{m_3} & \underline{V}_2^{m_3} & \underline{V}_3^{m_3} \end{bmatrix} \tag{24}$$

where underlined quantities are Fourier coefficients at frequency ω_c.

After obtaining the measurements, the decentralized specifications for (19) are applied. The results are given in Fig. 22 and marked with the "×" marker. Additionally, analytical results from Fig. 12 are given for the sake of comparison. Note that analytical results are not needed to apply the proposed decentralized specifications, and specifications can be applied directly to the black-box measurements. From Fig. 22 we can conclude that converter 1 satisfies the specifications, while converters 2 and 3 do not. The specifications are violated in the frequency range around 200 Hz which correlates with the frequency of the observed oscillations in Fig. 19.

To satisfy the specifications, the bandwidth of the current and voltage control loops of converter 2 is lowered to 250 and 40 Hz, and the parallel RC damper with values of $C_d = 1.3\text{mF}$ and $R_d = 2.2\Omega$ is added to the converter 3 input. After the changes are made, the specifications for all converters are satisfied. The resulting system is stable with all converters turned ON, as shown in Fig. 23.

Finally, to further validate the proposed method, the system's response is tested under step load changes. Specifically, the system is examined in a scenario where all converters meet the given specifications. The load of each converter is increased by approximately 20% by connecting an additional resistor in parallel with the existing load resistor. The results, presented in Fig. 24, confirm that the converters exhibit different transient responses due to differences in their control and output filter parameters. This demonstrates that while the proposed decentralized specifications ensure system stability, they do not provide explicit performance metrics such as settling time, overshoot, or disturbance rejection. Therefore, converter designers should aim to meet the given specifications while also achieving the

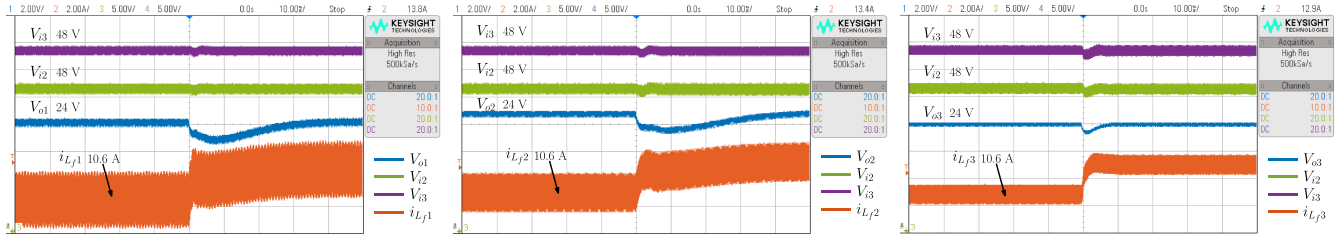

(a) (b) (c)

Fig. 24. Load step transient response of the system with all converters satisfying the specifications. Load is increased by 20%. (a) Converter 1. (b) Converter 2. (c) Converter 3.

desired performance. This can be seen as a limitation of the proposed method, and an analysis of the relationship between the proposed specifications and the performance of converters is a potential area for future research.

V. Conclusion

This article proposes a novel method to impose decentralized specifications on individual converters connected to the different nodes of a dc distribution grid. To enable this, particular partitioning that groups converters, which we want to impose specifications on, in one subsystem, while leaving the rest of the grid in the other, was utilized. This partitioning ensures that the minor loop gain structure is well-suited for the derivation of decentralized specifications. Furthermore, the inputs and outputs of individual subsystems are picked such that minor loop gain does not contain the RHP poles. For the first time, the Gershgorin theorem was used to derive decentralized specifications for the complex multinode dc system. To reduce the conservativeness of the proposed specifications, an additional combination with the passivity theorem was also proposed. Resulting specifications are computationally efficient and straightforward to apply, as they are represented by simple frequency domain expressions, which makes them applicable to large-scale systems. Verification of proposed specifications was performed experimentally on an application example composed of three buck converters connected with cables. It is shown that specifications are easily applicable both on analytical models and black-box impedance measurements, and that satisfaction of specifications is sufficient for system stability. Finally, time-domain instability is observed in the case when specifications are not satisfied. This instability is successfully mitigated by modifying converters such that specifications are satisfied.

Appendix A

In this appendix, it is proven that the combination of the Gershgorin and passivity-based specifications (19) is sufficient for the stability of the system.

First, the transfer function $\mathbf{C}(j\omega)$ is said to be passive at frequency ω_c if

$$\mathbf{C}(j\omega_c) + \mathbf{C}^H(j\omega_c) > 0 \tag{25}$$

where $\mathbf{C}^H(j\omega_c)$ is the Hermitian complex conjugate transpose of $\mathbf{C}(j\omega_c)$. Since $\mathbf{C}(j\omega)$ is a diagonal matrix, the passivity condition at frequency ω_c is equal to

$$\forall k \in \{1, 2, \ldots, n\} \quad \mathrm{Re}\{C_k(j\omega_c)\} > 0. \tag{26}$$

If both $\mathbf{C}(s)$ and $\mathbf{G}(s)$ are passive at ω_c, eigenlocies of loop gain $\lambda(\mathbf{L}(j\omega_c))$, $\mathbf{L}(j\omega_c) = \mathbf{C}(j\omega_c)\mathbf{G}(j\omega_c)$ are not located on half-line from (0,0) to $(-\infty, 0)$.

To prove this the properties of numerical range of a matrix will be used. The numerical range of a complex matrix $\mathbf{C}^\omega = \mathbf{C}(j\omega_c)$ is defined as

$$W(\mathbf{C}^\omega) = \{x^H \mathbf{C}^\omega x \mid x \in \mathbb{C}^n, \|x\| = 1\}. \tag{27}$$

By using the properties of the numerical range, phases of the matrix are defined by using sectorial decomposition [22] and are labeled as

$$\overline{\phi}(\mathbf{C}^\omega) = \phi_1(\mathbf{C}^\omega) \geq \phi_2(\mathbf{C}^\omega) \geq \ldots \geq \phi_n(\mathbf{C}^\omega) = \underline{\phi}(\mathbf{C}^\omega). \tag{28}$$

If the $\mathbf{C}(j\omega)$ matrix is passive at ω_c, then the phases of the $\mathbf{C}^\omega = \mathbf{C}(j\omega_c)$ are inside the $(-\pi/2, \pi/2)$ interval [22].

Another theorem states that if we have two matrices $\mathbf{C}^\omega = \mathbf{C}(j\omega_c)$ and $\mathbf{G}^\omega = \mathbf{G}(j\omega_c)$ then we can say this about the eigenlocies of the product $\mathbf{L}(j\omega_c) = \mathbf{C}^\omega\mathbf{G}^\omega$ [22]

$$\underline{\phi}(\mathbf{C}^\omega) + \underline{\phi}(\mathbf{G}^\omega) \leq \angle\lambda_i(\mathbf{C}^\omega\mathbf{G}^\omega) \leq \overline{\phi}(\mathbf{C}^\omega) + \overline{\phi}(\mathbf{G}^\omega). \tag{29}$$

If both $\mathbf{C}^\omega = \mathbf{C}(j\omega_c)$ and $\mathbf{G}^\omega = \mathbf{G}(j\omega_c)$ are passive, then the eigenlocies of $\mathbf{L}(j\omega_c)$ are not located on the half-line from (0,0) to $(-\infty, 0)$, since the angles of the eigenlocies are inside the $(-\pi, \pi)$ interval (29).

Since the specifications derived using Gershgorin theorem (16) used the forbidden region which is the subset of the half-line from (0,0) to $(-\infty, 0)$, then the eigenlocies of the loop gain $\mathbf{L}(j\omega_c)$ will not enter the forbidden region if all converters are passive, but not satisfying the Gershgorin theorem specifications. This is sufficient for the stability of the system.

References

[1] Y. Cheng et al., "Real-world subsynchronous oscillation events in power grids with high penetrations of inverter-based resources," *IEEE Trans. Power Syst.*, vol. 38, no. 1, pp. 316–330, Jan. 2023.

[2] X. Wang and F. Blaabjerg, "Harmonic stability in power electronic-based power systems: Concept, modeling, and analysis," *IEEE Trans. Smart Grid*, vol. 10, no. 3, pp. 2858–2870, May 2019.

[3] N. Pogaku, M. Prodanovic, and T. C. Green, "Modeling, analysis and testing of autonomous operation of an inverter-based microgrid," *IEEE Trans. Power Electron.*, vol. 22, no. 2, pp. 613–625, Mar. 2007.

[4] A. Riccobono and E. Santi, "Comprehensive review of stability criteria for DC power distribution systems," *IEEE Trans. Ind. Appl.*, vol. 50, no. 5, pp. 3525–3535, Sep. 2014.

[5] R. D. D. Middlebrook, "Input filter consideration in design and application of switching regulators," *in Proc. IEEE Ind Appl. Soc Annu Meet.*, 1976, pp. 366–382.
[6] J. Sun, "Impedance-based stability criterion for grid-connected inverters," *IEEE Trans. Power Electron.*, vol. 26, no. 11, pp. 3075–3078, Nov. 2011.
[7] B. He, W. Chen, X. Ruan, X. Zhang, Z. Zou, and W. Cao, "A generic small-signal stability criterion of DC distribution power system: Bus node impedance criterion (BNIC)," *IEEE Trans. Power Electron.*, vol. 37, no. 5, pp. 6116–6131, May 2022.
[8] H. Zhang, X. Wang, M. Mehrabankhomartash, M. Saeedifard, Y. Meng, and X. Wang, "Harmonic stability assessment of multiterminal DC (MTDC) systems based on the hybrid AC/DC admittance model and determinant-based GNC," *IEEE Trans. Power Electron.*, vol. 37, no. 2, pp. 1653–1665, Feb. 2022.
[9] H. Zhang, M. Mehrabankhomartash, M. Saeedifard, Y. Zou, Y. Meng, and X. Wang, "Impedance analysis and stabilization of point-to-point HVdc systems based on a hybrid ac–dc impedance model," *IEEE Trans. Ind. Electron.*, vol. 68, no. 4, pp. 3224–3238, Apr. 2021.
[10] Y. Liao, X. Wang, and X. Wang, "Frequency-domain participation analysis for electronic power systems," *IEEE Trans. Power Electron.*, vol. 37, no. 3, pp. 2531–2537, Mar. 2022.
[11] Y. Li et al., "Stability analysis and location optimization method for multiconverter power systems based on nodal admittance matrix," *IEEE J. Emerg. Sel. Top. Power Electron.*, vol. 9, no. 1, pp. 529–538, Feb. 2021.
[12] D. Yang and Y. Sun, "SISO impedance-based stability analysis for system-level small-signal stability assessment of large-scale power electronics-dominated power systems," *IEEE Trans. Sustain. Energy*, vol. 13, no. 1, pp. 537–550, Jan. 2022.
[13] Y. Zhan, X. Xie, H. Liu, H. Liu, and Y. Li, "Frequency-domain modal analysis of the oscillatory stability of power systems with high-penetration renewables," *IEEE Trans. Sustain. Energy*, vol. 10, no. 3, pp. 1534–1543, Jul. 2019.
[14] C. Zhang, H. Zong, X. Cai, and M. Molinas, "On the relation of nodal admittance- and loop gain-model based frequency-domain modal methods for converters-dominated systems," *IEEE Trans. Power Syst.*, vol. 38, no. 2, pp. 1779–1782, Mar. 2023.
[15] Y. Zhu, Y. Gu, Y. Li, and T. C. Green, "Impedance-based root-cause analysis: Comparative study of impedance models and calculation of eigenvalue sensitivity," *IEEE Trans. Power Syst.*, vol. 38, no. 2, pp. 1642–1654, Mar. 2023.
[16] L. Huang et al., "Gain and phase: Decentralized stability conditions for power electronics-dominated power systems," *IEEE Trans. Power Syst.*, vol. 39, no. 6, pp. 7240–7256, Nov. 2024.
[17] X. Feng, J. Liu, and F. Lee, "Impedance specifications for stable DC distributed power systems," *IEEE Trans. Power Electron.*, vol. 17, no. 2, pp. 157–162, Mar. 2002.
[18] X. Wang et al., "Decentralized impedance specifications for small-signal stability of DC distributed power systems," *IEEE J. Emerg. Sel. Top. Power Electron.*, vol. 5, no. 4, pp. 1578–1588, Dec. 2017.
[19] C. Zhang, W. Chen, and B. He, "Decentralized impedance specifications for paralleled DC distribution power system with multiple-voltage-level buses," *IEEE Trans. Power Electron.*, vol. 39, no. 1, pp. 112–124, Jan. 2024.
[20] L. Stojanović, R. Cvetanović, P. Mattavelli, S. Buso, and D. Biaene, "Decentralized impedance specifications for grid-connected converters in AC grids," in *Proc. Energy Convers. Congr. Expo Europe*, 2024, pp. 1–7.
[21] D. Zhao, W. Chen, and L. Qiu, "When small gain meets small phase," Feb. 2022. [Online]. Available: https://arxiv.org/abs/2201.06041
[22] D. Wang, W. Chen, S. Z. Khong, and L. Qiu, "On the phases of a complex matrix," *Linear Algebra Appl.*, vol. 593, pp. 152–179, May 2020.
[23] C. A. Desoer and M. Vidyasagar, *Feedback systems: Input-output properties*. Philadelphia, PA, USA: SIAM, 2009.
[24] F. Liu, J. Liu, H. Zhang, and D. Xue, "Stability issues of $Z + Z$ type cascade system in hybrid energy storage system (HESS)," *IEEE Trans. Power Electron.*, vol. 29, no. 11, pp. 5846–5859, Nov. 2014.
[25] Y. Ren, R. Duan, L. Chen, W. Huang, C. Wu, and Y. Min, "Stability assessment of grid-connected converter system based on impedance model and Gershgorin theorem," *IEEE Trans. Energy Convers.*, vol. 35, no. 3, pp. 1559–1566, Sep. 2020.
[26] D. Van De Sype, K. De Gusseme, A. Van Den Bossche, and J. Melkebeek, "Small-signal Laplace-domain analysis of uniformly-sampled pulse-width modulators," in *Proc. IEEE 35th Annu. Power Electron. Spec. Conf.*, 2004, pp. 4292–4298.

Lazar Stojanović (Student Member, IEEE) was born in Belgrade, Serbia, in 1999. He received the B.S. and M.S. degrees in electrical engineering from the University of Belgrade, Belgrade, Serbia, in 2021 and 2022, respectively. Since 2022, he has been working toward the Ph.D. degree in control and impedance specifications for grid-connected converters with the Power Electronics Group, Department of Management and Engineering, University of Padova, Vicenza, Italy.

His research interests include modeling, control, and impedance specifications of grid-connected converters for both ac and dc grids.

Ružica Cvetanović (Graduate Student Member, IEEE) was born in Belgrade, Serbia, in 1996. She received the B.S. and M.S. degrees from the University of Belgrade, Belgrade, Serbia, in 2019 and 2020, respectively, and the Ph.D. degree from the University of Padova, Padua, Italy, in 2025, all in electrical engineering.

From 2020 to 2021, she worked with the Power Converters and Systems Group, School of Electrical Engineering, University of Belgrade. In 2021, she joined the Power Electronics Group, Department of Information Engineering, University of Padova, as a Visiting Researcher. Her research interests include modeling and digital control of grid-tied power electronics converters.

Paolo Mattavelli (Fellow, IEEE) received the M.S. (Hons.) and Ph.D. degrees in electrical engineering from the University of Padova, Padova, Italy, in 1992 and 1995, respectively.

He is currently a Full Professor in electronics with the University of Padova. His major research interests include analysis, modeling, and control of power converters, grid-connected converters for renewable energy systems and microgrids, and high-temperature and high-power-density power electronics.

Dr. Mattavelli was an Associate Editor for IEEE TRANSACTIONS ON POWER ELECTRONICS from 2003 to 2012. His current Google scholar H-index is 81. He is a Coeditor-in-Chief for IEEE TRANSACTIONS ON POWER ELECTRONICS. From 2005 to 2010, he was the Industrial Power Converter Committee Technical Review Chair for IEEE Transactions on Industry Applications. For the terms 2003–2006, 2006–2009, and 2013–2015, he was a Member-at-large of the IEEE Power Electronics Society's Administrative Committee. He was a recipient of the Prize Paper Award in IEEE Transactions on Power Electronics in 2005, 2006, 2011, and 2012, and the 2nd Prize Paper Award at the IEEE Industry Applications Society Annual Meeting in 2007.

Simone Buso (Member, IEEE) received the M.Sc. degree in electronic engineering and the Ph.D. degree in industrial electronics from the University of Padova, Padova, Italy, in 1992 and 1997, respectively.

He is currently an Associate Professor of electronics with the Department of Information Engineering (DEI), University of Padova. His main research interests include the industrial and power electronics fields and are related specifically to switching converter topologies, digital control of power converters, renewable energy sources, and smart micro-grids.